

Detecting Parkinson's Disease from a Speech-task in an Accessible and Interpretable manner

WASIFUR RAHMAN, University of Rochester, USA

SANGWU LEE, University of Rochester, USA

MD. SAIFUL ISLAM, Bangladesh University of Engineering and Technology, Bangladesh

ABDULLAH AL MAMUN, University of Rochester, USA

VICTOR ANTONY, University of Rochester, USA

HARSHIL RATNU, University of Rochester, USA

MOHAMMAD RAFAYET ALI, University of Rochester, USA

EHSAN HOQUE, University of Rochester, USA

Every nine minutes a person is diagnosed with Parkinson's Disease (PD) in the United States. However, studies have shown that between 25 and 80% of individuals with Parkinson's Disease (PD) remain undiagnosed. An online, in the wild audio recording application has the potential to help screen for the disease if risk can be accurately assessed. In this paper, we collect data from 726 unique subjects (262 PD and 464 Non-PD) uttering the "quick brown fox jumps over the lazy dog ..." to conduct automated PD assessment. We extracted both standard acoustic features and deep learning based embedding features from the speech data and trained several machine learning algorithms on them. Our models achieved 0.75 AUC by modeling the standard acoustic features through the XGBoost model. We also provide explanation behind our model's decision and show that it is focusing mostly on the widely used MFCC features and a subset of dysphonia features previously used for detecting PD from verbal phonation task.

Additional Key Words and Phrases: Parkinson's disease, Datasets, Neural Networks, Machine Learning, Audio Classification, Audio Processing, Speech Recognition, Accessible, Remote, MDS-UPDRS

ACM Reference Format:

Wasifur Rahman, Sangwu Lee, Md. Saiful Islam, Abdullah Al Mamun, Victor Antony, Harshil Ratnu, Mohammad Rafayet Ali, and Ehsan Hoque. 2020. Detecting Parkinson's Disease from a Speech-task in an Accessible and Interpretable manner. 1, 1 (September 2020), 19 pages. <https://doi.org/10.1145/nnnnnnn.nnnnnnn>

1 INTRODUCTION

Parkinson's disease (PD) is the second most common neurodegenerative disease [11], with an estimate of more than one million people in North America alone to be affected [23]. Sadly, there is no cure for such a prevalent disease, but medication can alleviate the symptoms significantly if the patient is diagnosed early [39]. A standard diagnosis requires the patient consulting a neurologist who administers a specific set of tasks involving speech, movement, and other mental and physical activities. However, not every people has access to a neurologist. According to a study of 2013 [21], there were only 1,200 neurologists in India, for a population of nearly 1.3 billion. More than 20% PD patients remain undetected [37], and thereby cannot be treated. Imagine the scenario,

Authors' addresses: Wasifur Rahman, echowdh2@ur.rochester.edu, University of Rochester, USA; Sangwu Lee, slee232@u.rochester.edu, University of Rochester, USA; Md. Saiful Islam, saiful.11722@gmail.com, Bangladesh University of Engineering and Technology, Bangladesh; Abdullah Al Mamun, amamun@u.rochester.edu, University of Rochester, USA; Victor Antony, vantony@u.rochester.edu, University of Rochester, USA; Harshil Ratnu, hrtatnu@u.rochester.edu, University of Rochester, USA; Mohammad Rafayet Ali, mali7@cs.rochester.edu, University of Rochester, USA; Ehsan Hoque, mehoque@cs.rochester.edu, University of Rochester, USA.

2020. XXXX-XXXX/2020/9-ART \$15.00
<https://doi.org/10.1145/nnnnnnn.nnnnnnn>

where any person can be diagnosed for PD right away, just by visiting a website. In this paper, we make a small step towards a remote system for PD diagnosis with a focus of making it accessible to any person in the world.

Due to the ubiquity of electronic devices, Internet, and advancement in technology, researchers are focusing on detecting the symptoms of PD remotely. Recent studies show that, symptoms involving speech and motor functions can be detected with clinical accuracy using statistical regression and machine learning techniques [3, 25, 36]. Wearable sensor data has been analyzed to detect movement cues [28, 47]. Non-invasive systems based on posed and spontaneous facial expressions have also been explored [4, 18, 41, 49]. While researchers are trying to detect PD based on multitude of remote tasks, significant progress has been made in speech-related tasks because of the ubiquity of audio recording hardware and ease of performing these tasks. Also, studies report that around 90% of PD patients exhibit vocal impairment [16, 27] and it can be one of the earliest indicators of PD [12].

Dysphonia (distortion or abnormality of voice), dysarthria (problems with speech articulation), and hypophonia (reduced voice volume) are voice disorders highly associated with PD. Two speech tasks are very popular for detecting these disorders: (i) sustained phonation (the subject is supposed to utter a single vowel for a long time with constant pitch), and (ii) running speech (the subject speaks a standard sentence, like “the quick brown fox jumps over the lazy dog”). Max et al. [25] worked with automatic detection of dysphonia leading to correctly classifying people with PD from the healthy ones. Tsanas et al. [43] focus on the telemonitoring of self-administered sustained vowel phonations task to predict the UPDRS rating, a popular indicator of PD symptoms. These studies train their systems based on data captured by advanced devices (e.g., wearable devices, high resolution video recorder, Intel AHTD telemonitoring system) that are not accessible by common people. The performance of these systems degrade significantly when predicting on data collected in home acoustics [35]. Although Poorjam et al. [35] develop automated techniques to remove noise from audios recorded in home acoustics, their algorithms are designed only for the sustained phonations task, and cannot be used for the running speech task where the noise is more unpredictable.

In this paper, we focus on the wide accessibility of remote PD detection systems since the disease does not care about the patient having access to a neurologist or advanced devices. We argue that, an web application that can assess PD symptoms remotely and requires only an internet connected device with integrated camera and microphone, is more accessible and convenient to common people, even living in the rural areas. Also, we observe that the running speech task being similar to regular conversation, requires less supervision than the sustained phonation task. So, in this paper, we focus on detecting PD based on the running speech task. We collect speech recordings of 726 subjects (262 diagnosed with PD) in an uncontrolled, wild settings through a website named ParkTest¹, and employ popular machine learning algorithms to classify subjects with PD from the healthy ones. Although Parkinson’s disease is mostly associated with older people, the age of our subjects varies from 15 to 90, so that the model can be used for younger people as well. We extract traditional PRAAT features [6] and other non-traditional features like DFA, RPDE, PPE, etc., that are reported to perform better than the traditional features [25]. To the best of our knowledge, we are the first to analyze the self-supervised running speech task in the wild. Although such a task is very challenging, we are encouraging it because the running speech task is very similar to regular conversation. If a model can be trained to do well in this task, there remains a good possibility of detecting PD from regular conversation, which would be much more helpful, especially for the people who find it difficult to follow instructions. In this regard, our model looks promising, by achieving **0.7533 AUC** (the AUC of a random predictor is 0.5). We hope, this work will inspire contributions from the researchers towards developing a remote system for detecting Parkinson’s disease, easily accessible by any person in the world.

Table 1. Demographic Composition of our Dataset

	PD	Non-PD
N	262	464
Female/Male	101/161	300/164
Age (mean \pm std)	65.92 \pm 9.16	57.98 \pm 14.21
Country (US/other)	199/63	419/45
Years since diagnosed (mean \pm std)	7.88 \pm 5.41	N/A

2 RESULTS

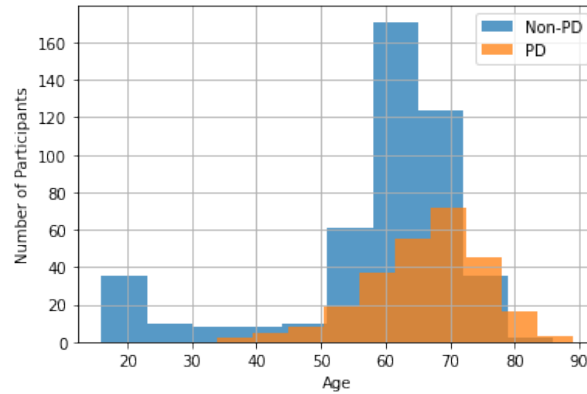


Fig. 1. A bar plot showing age-distribution of PD and Non-PD subjects in our dataset. Although the number of non-PD subjects is 1.8 times the number of PD subjects, there is a healthy balance between these two groups in the age-range of [40-80] years. However, Non-PD subjects outnumber their PD counterparts in the age group [20-40]. Similarly, PD subjects outnumber Non-PD subjects significantly in the age group of [80-90] years.

2.1 Data Preparation

We collected data from 726 unique subjects uttering the sentences *“The quick brown fox jumps over the lazy dog. The dog wakes up and follows the fox into the forest, but again the quick brown fox jumps over the lazy dog”* using the Parkinson’s Analysis with Remote Kinetic-tasks (PARK) [24] tool. Table 1 gives a detailed account of the subjects and Fig 1 denotes how the age distribution is for both the PD and non-PD patients. Only 54 data-points were collected in the Lab-environment under the supervision of the doctors; the other 672 data-points were collected by the subjects themselves in their Home-environment with guidance from the PARK tool. The data was pre-processed and both standard acoustic features and deep-learning based audio Embedding features were extracted – we will call them *Standard-features* and *Embedding-features* from now on. A complete list of *Standard-features* features is provided in Table 2 followed by a detailed description of the features in 4.3. We extract the *Embedding-features* from PASE encoder [33] that converts an audio signal into a representative vector.

¹<https://parktest.net/>

Table 2. Names of all the features, feature collection protocol and short-description of the features used by us. The correlated features were removed and features marked with * were used in building the models. Feature names are preceded by the loosely defined umbrella category they belong to.

Feature	Code source	Short-description
Pitch:f0m*	[26]	Median Frequency
Pitch:meanF0Hz*	[6]	Mean Frequency
Pitch:f0std*	[26]	Standard deviation in F0
Jitter:f0j*	[26]	Perturbation in F0 (mean variation)
Jitter:f0jr*	[26]	Perturbation in F0 (median variation)
Jitter:localJitter	[6]	Jitter variant
Jitter:localabsoluteJitter*	[6]	Jitter variant
Jitter:rapJitter	[6]	Jitter variant
Jitter:ppq5Jitter	[6]	Jitter variant
Jitter:ddpJitter*	[6]	Jitter variant
Shimmer:ash	[26]	Amplitude perturbation (using mean)
Shimmer:ashr*	[26]	Amplitude perturbation (using median)
Shimmer:localShimmer	[6]	Shimmer variant
Shimmer:localdbShimmer	[6]	Shimmer variant
Shimmer:apq3Shimmer	[6]	Shimmer variant
Shimmer:apq5Shimmer	[6]	Shimmer variant
Shimmer:apq11Shimmer*	[6]	Shimmer variant
Shimmer:ddaShimmer*	[6]	Shimmer variant
MFCC:cep[0-12]*	[26]	13 features of Mean MFCC
MFCC:cepj[0-12]*	[26]	13 features of Mean variation of MFCC
relbandpower[0-3]*	[46]	Four features capturing relative band power in four spectrum ranges
Harmonic to Noise ratio(HNR*)	[6]	Signal-to-noise ratio
Recurrence period density entropy(RPDE)*	[26]	F0 estimation uncertainty
Detrended Fluctuation Analysis(DFA)*	[26]	Measure of stochastic self-similarity in turbulent noise
Pitch period entropy (PPE*)	[25]	Measure of inability of maintaining constant F0

Table 3. *Home-environment and Lab-environment data*: The performance of various machine learning algorithms using the Standard-features and Embedding-features on a dataset combining data from both Home-environment and Lab-environment. We can see that the models using Standard-features perform better than the models using Embedding-features in terms of both Binary Accuracy and AUC. Although the model's perform similarly in using the Standard-features, XGBoost outperforms others by considering both the AUC and Accuracy metrics.

Algorithm	Standard-features		Embedding-features	
	AUC	Accuracy	AUC	Accuracy
SVM	0.7507	0.7355	0.7379	0.6915
Random Forest	0.745	0.7204	0.7259	0.708
LightGBM	0.7533	0.7204	0.7373	0.6928
XGBoost	0.7502	0.741	0.7219	0.6887

2.2 Detection of Parkinson's Disease on combined dataset of Home-environment and Lab-environment

To detect the PD patients from our combined dataset of Home-environment and Lab-environment data, we applied a standard set of machine learning algorithms like Support-vector-machine (SVM) [9], XGBoost [8], LightGBM [20], and Random-Forest [17]. We used a leave-one-out cross validation training strategy : each data

Table 4. The performance of various machine learning algorithms using the Standard-features and Embedding-features on the Home-environment data as the test set. The models were trained on both Home-environment and Lab-environment data, but the performance metrics are calculated on the Home-environment data only. The models using Standard-features perform better than their counterparts using Embedding-features in terms of both Binary Accuracy and AUC. Although the model’s perform similarly in using the Standard-features, XGBoost outperforms others by considering both the AUC and Accuracy metrics. However, the performance is slightly lower than the XGBoost model that uses both Home and Lab environment data in the test set:0.0123 in AUC and 0.004 in Accuracy

Algorithm	Standard-features		Embedding-features	
	AUC	Accuracy	AUC	Accuracy
SVM	0.7368	0.7336	0.7265	0.6964
Random Forest	0.7317	0.7173	0.7194	0.7143
LightGBM	0.7317	0.7173	0.7327	0.6979
XGBoost	0.7379	0.7366	0.7165	0.6949

Table 5. The performance of various machine learning algorithms using the Standard-features and Embedding-features on the Home-environment data. The SVM model using the Standard-features performs better than all other model combinations and the performance is quite similar to that of the previous models that uses both Home and lab environment data (Table 3)

Algorithm	Standard-features		Embedding-features	
	AUC	Acc.	AUC	Acc.
SVM	0.7354	0.7381	0.7288	0.6949
Random Forest	0.7208	0.7188	0.7083	0.692
LightGBM	0.7328	0.7158	0.7232	0.7054
XGBoost	0.7326	0.7113	0.705	0.6935

instance of the dataset is left out and the other n-1 instances are used to create a model and predict the left-out instance iteratively. We used metrics like Binary Accuracy and Area-Under-Curve (AUC) to report our model’s performance. Since our dataset is imbalanced, AUC is a much better metric to understand the true performance of our models.

Table 3 contains the results of applying various machine learning algorithms on both the *Standard-features* and *Embedding-features*. Applying XGBoost on the Standard-features give us the best performance of 0.7502 AUC and 0.741 Accuracy (baseline AUC for random prediction is 0.5 and baseline Accuracy of predicting the Non-PD majority class is 0.64). We also notice that models utilizing the Standard-Features works better than those utilizing the deep learning based techniques like PASE. The performance of various models are very consistent, which implies that much of the predictive power is coming from the features, and not from the particular modeling technique employed.

2.3 Model Interpretation

For recognizing the features that are driving our model’s performance, we are using the SHAP (SHapley Additive exPlanations) [29, 30] technique. Shapley value is a game-theoretic concept of distributing the payout fairly among the players [38]. In the machine learning context, each individual feature of a data instance can be thought of as a player and the payout is the difference between an instance’s prediction and average prediction. SHAP creates a local explanation for an individual data instance as outlined in Fig. 2. For each instance, it explains the magnitude and direction of each feature’s impact on the model’s output value. Then we aggregate all these local explanations and creates a global interpretation for the entire dataset (as outlined in Fig. 3).

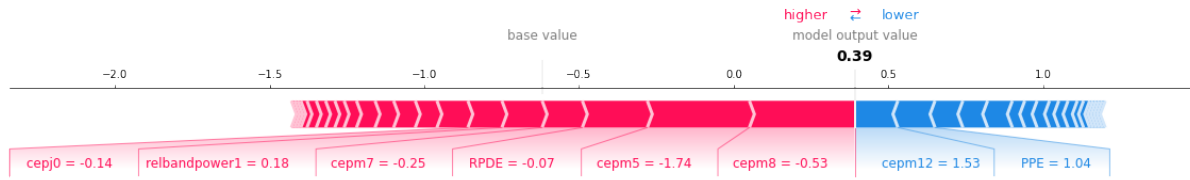


Fig. 2. SHAP analysis of an individual subject. The subject is a PD patient and the model correctly identified him as such. In the plot, the features colored in red are pushing the model towards predicting higher value and predicting the subject to be a PD patient. Conversely, the blue colored features are pushing the model towards predicting lower value for the subject.

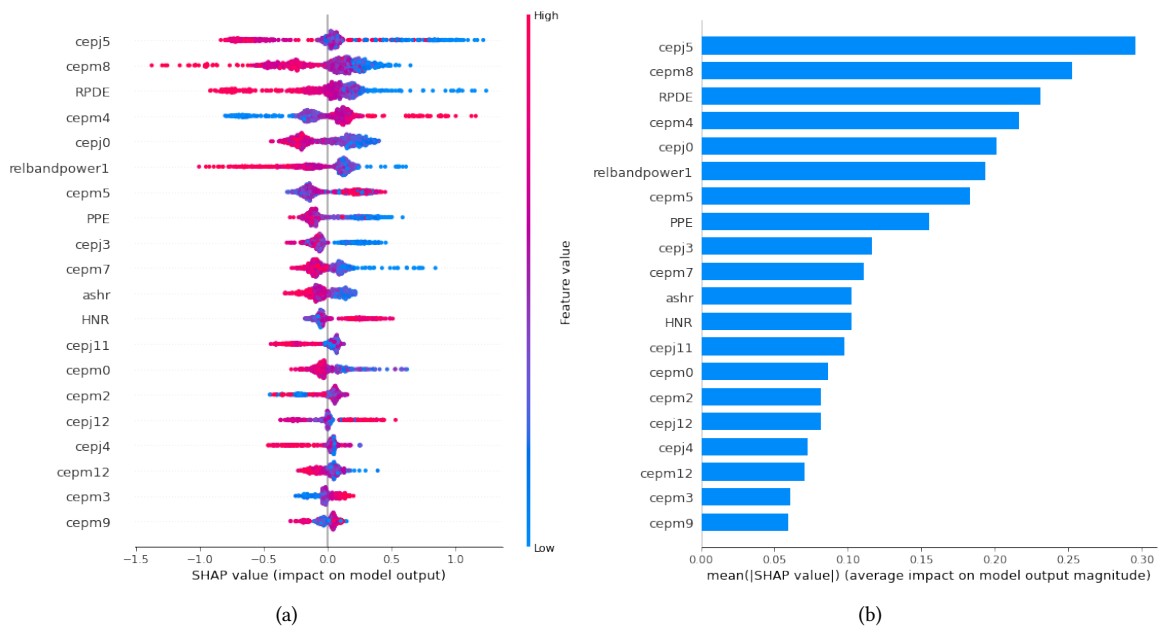


Fig. 3. SHAP analysis of our model on all data: This figure depicts the most important features for a model by plotting the SHAP values of every feature in every data sample. Plot (a) arranges the features in two steps: (i) Sorts features by the sum of SHAP value magnitudes over all samples, (ii) Uses SHAP values to show a distribution of how each feature impacts the model's output: red color represents high value of a feature, blue represents low. For example, higher values of the feature cepm13 (the second to last one) increases the model's output value. Plot (b) sorts all features by their mean absolute value to create a standard bar plot. From both plots, we see that the most salient features are usually the MFCC features : mean MFCC values in each channel is represented by the prefix cepm and the variation in those channels by cepj. Apart from that, features like RPDE (measuring uncertainty in F0 estimation), PPE (measure of inability of maintaining a constant F0), HNR (Harnomic to noise ratio), ashhr (median in amplitude perturbation), realbandpower1 (amount of power in the frequency range 0.5-1kHz) also impact the model's behaviour.

2.3.1 Model Interpretation Results. In Fig. 3.a each feature is ranked by its mean absolute SHAP value; irrespective of whether the value is positive or negative. On the other hand, Fig. 3.b shows how both the magnitude and direction (positive/negative) of each feature's value are impacting the model's decision. In both cases, we can clearly see that the features that are impacting the model's performance are typically the spectral features: the mean values (represented by the prefix *cep*m) or the variance of MFCC (represented by the prefix *cep*j). Apart from that, some other complex features like RPDE (measuring uncertainty in F0 estimation), PPE (measure of inability of maintaining a constant F0), HNR (Harmonic to noise ratio) also impact the model's decision.

MFCC have already proven to be a useful audio feature in a wide range of audio tasks like speaker recognition [5], speech recognition [10], music information retrieval like genre classification, audio similarity measures [31], voice activity detection [22]. Besides, they have also been successfully used adopted for voice quality assessment [44]. However, as MFCC essentially denotes how energy is distributed in each of the buckets of frequency domain, it is difficult to relate the SHAP values with the physical interpretation of those features.

Besides, upon a close inspection of [25], the probability distribution of HNR, RPDE, DFA and PPE all have significant overlap among them and therefore, it actually makes sense that SHAP features also have a significant overlap. The high impact on HNR, RPDE and PPE on the model's output is in congruence with the findings by Little et al. [25]. HNR denotes the Harmonic-to-Noise Ratio, RPDE measures the variation in periodicity of voice signals, and PPE measures the inability of a speaker to maintain a constant F0. A typical healthy person should have high HNR, low RPDE and low PPE in the verbal phonation task – the task for pronouncing 'AHHH' – for data collected through a standardized device like Intel AHTD [25]. However, Little et al. also demonstrated that there is often significant overlap in probability distribution for each of these features between the PD and Non-PD voice data [25]. Upon close examinations, we see that in our case, there are lots of overlaps in terms on SHAP values in for these three features – exemplified by the mixed colors around SHAP values close to zero (either positive or negative). Besides, according to our SHAP analysis, the model's output value is increased by: lower values of RPDE, lower values of PPE and higher values of HNR are increasing the model's output value. All these findings are incongruent with those of Little et al. [25]. However, the intuition behind both the RPDE and PPE are derived for the verbal phonation task by assuming that the healthy subjects will be able to maintain a smooth and pseudo-periodic voice pattern. But uttering multiple sentences introduces a lot of variation in the data and hence a lot more nuanced patterns to deal with. Therefore, the intuitions behind those features does not carry while uttering multiple sentences. However, we can still see that those features are important in determining PD from speech tasks. Therefore, further research is necessary to augment those features to work well in the speech task. In the case of HNR, our data contains a lot of outside noise from TV, other people, or the microphone, which may be contributing to the behavior of SHAP value for HNR.

2.3.2 Interpretation validation. As SHAP constructs individual local interpretation and then provides an aggregated view of the results, we want to validate the results of the SHAP model. In order to do that, we took the features depicted in Fig 3 in terms of their decreasing SHAP value and incrementally added them one by one in the feature set. For each feature set, we trained a new model and reported the performance in terms of AUC and Accuracy. As depicted in Fig. 4 through a three-point moving average trend-line, the value of AUC plateaued after we added 10 features. Thus, we can show that, SHAP can recognize the most features driving the model's performance.

2.4 Predicting PD from Home-environment data only

2.4.1 Removing Lab-environment data from Test set. In Table 4, we present the results on Home-environment data by removing the Lab-environment data from test set. As we are using leave-one-out-cross-validation, we have predictions on every data instance. We can see that the results exhibit almost the same pattern as in Table 3. We are still getting the best performance using the Acoustic-features and the various models are performing

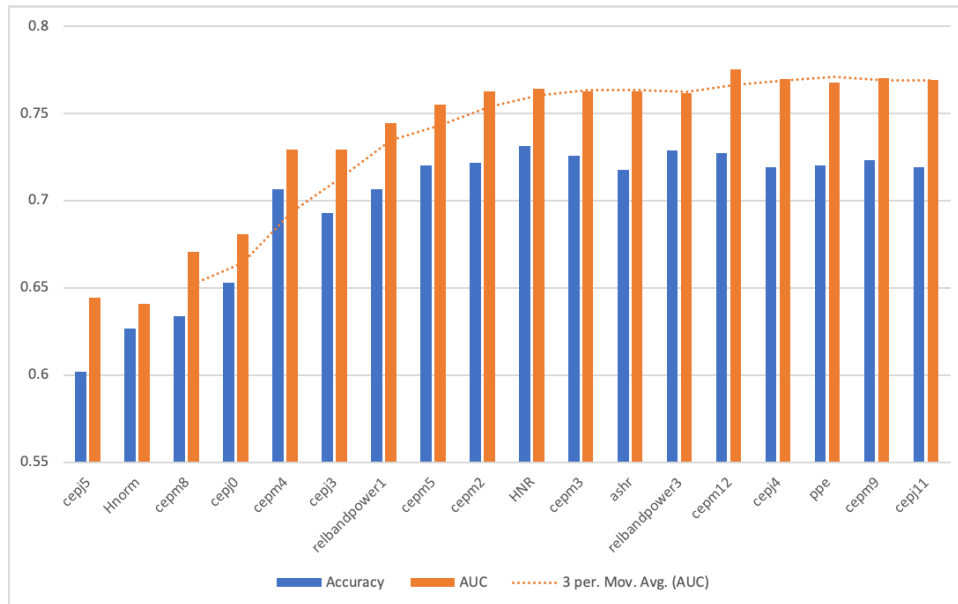


Fig. 4. Validating the SHAP output of Fig. 3: We started with the most important feature depicted in Fig.3 (cepj5) and added the next salient feature one at a time. For each feature set, we trained a new model and showed that model’s performance in terms of AUC and Accuracy. As evident from the Figure, after adding 10 most salient features (up to HNR), the primary metric, AUC’s value is saturated. We are showing a three-point moving average to demonstrate the saturation of AUC value.

almost the same. However, note that the test set of Table 3 and Table 5 are not the same, hence the results are not directly comparable. But the results demonstrate that our models’ performance do not get worse by excluding the Lab-environment data from test-set.

2.4.2 Training new model by excluding Lab-environment data. In Table 5, we present the results by training new models from the home-environment data only. From there, we can observe the same pattern observed in previous two analysis: We are still getting competitive performance from using Home-environment data only, Acoustic-features still outperforms the Embedding-features and the performance of the models are fairly consistent.

Table 6. Group-Specific-Performance: These scores are achieved after training the model on entire dataset and then checking the performance of the model on three separate groups: Male, Female and Age-matched. Age-matched group is constructed from people over 50 years old. We can see that the performance for each sub-group is in par with the performance on the entire dataset (Table 3), except for the Female group. This performance degradation can be attributed to the PD/Non-PD imbalance within the Female group (101 PD Vs. 300 Non-PD)

Algorithm	Male		Female		Age-matched	
	AUC	Accuracy	AUC	Accuracy	AUC	Accuracy
SVM	0.7751	0.7292	0.6741	0.7556	0.7543	0.7209
Random Forest	0.7554	0.7262	0.6893	0.7606	0.7466	0.7209
LightGBM	0.7461	0.6892	0.7238	0.7456	0.752	0.7039
XGBoost	0.7549	0.72	0.7127	0.7581	0.7421	0.7225

Table 7. Gender and age stratified models: Only male data is selected, separate model is trained on it. The female data is selected, separate model is trained on it. Then old people data are selected and separate model are trained on it

Algorithm	Male		Female		Age-matched	
	AUC	Accuracy	AUC	Accuracy	AUC	Accuracy
SVM	0.795	0.7169	0.6599	0.7631	0.7547	0.7225
Random Forest	0.7584	0.7015	0.6985	0.788	0.7399	0.7132
LightGBM	0.7254	0.6646	0.7173	0.7681	0.7498	0.7116
XGBoost	0.7617	0.7169	0.6821	0.7706	0.7419	0.7039

2.5 Gender and age Stratified Analysis

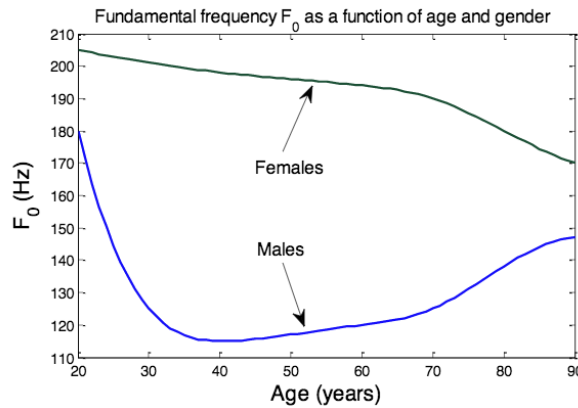


Fig. 5. Changes in fundamental frequency F_0 of voice as a function of gender and age (collected from Tsanas et al.[43], who took the inspiration of Titze et al. [42]). Female voices have higher F_0 value but it decreases with age. Males typically have higher F_0 value in their youth, with decreases with age and then increases roughly after the age of 45.

The characteristic of people's voice is greatly influenced of their age and gender. From Fig. 5, we can clearly see that Males and Females display a changing characteristics in their voice as they progress in age. Therefore, it

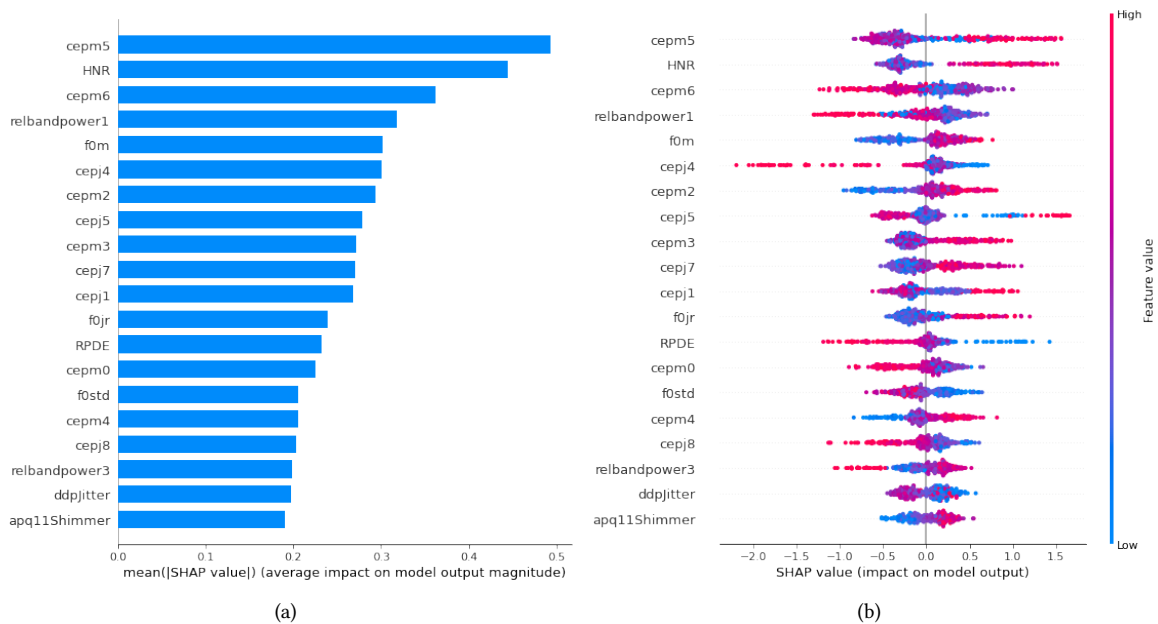


Fig. 6. SHAP for Female model: This figure depicts the most important features for the model using the Female data by plotting the SHAP values of every feature in every data sample. Plot (a) arranges the features in two steps: (i) Sorts features by the sum of SHAP value magnitudes over all samples, (ii) Uses SHAP values to show how each feature impacts the model’s output: red color represents high value of a feature, blue represents low. For example, higher values of the feature cepm13 (the second to last one) increases the model’s output value (b) Sorts all features by their mean absolute value to create a standard bar plot. From both plots, we see that the most impactful features are usually the MFCC features : mean MFCC values in each channel is represented by the prefix cepm and the variation in those channels by cepj. Apart from that features like RPDE (measuring uncertainty in F0 estimation), HNR (Harmonic to noise ratio), ashr (median in amplitude perturbation), relative-band-power features (relbandpower1 and relbandpower3 (amount of power in the frequency range 0.5-1kHz and 2kHz-4kHz) also impact the model’s behaviour. Besides, there are some influence from the Pitch related features as well (f0m,f0jr,f0std). Please refer to Table 2 for a complete list of features and 4.3 for a detailed description of features.

can produce a confounding effects in analyzing PD from audio where the model uses this information to detect PD, instead of finding the relevant features. To take care of that, researchers in the past adopted some standards. Tsanas et. al [45] analyzed data containing male and female subjects separately. Other researchers analyzed an aged matched data-sample by removing all people under the age of 50 from dataset [2, 24].

However, we built a single model inclusive of all genders for several reasons. First, an estimated 1.4 million people, 0.6% of the population in the US, is transgender [13]. By building a model that works for either male or female, we can potentially exclude these people from benefiting from our system. Second, dividing the dataset into two portions will reduce available training data for each model, which may in turn return the generalization capability of each model. Third, there are potential shared characteristics among vocal patterns of both gender that can be relevant for detecting PD.

Besides, our model analyzes data from patient of all ages. Although most people who are diagnosed with PD are over the age of 60, about 10%-20% of the diagnosed PD population are under the age of 50, and about half of them are under the age of 40 [1]. As an anecdotal evidence, Michel J Fox was diagnosed with PD at the age of

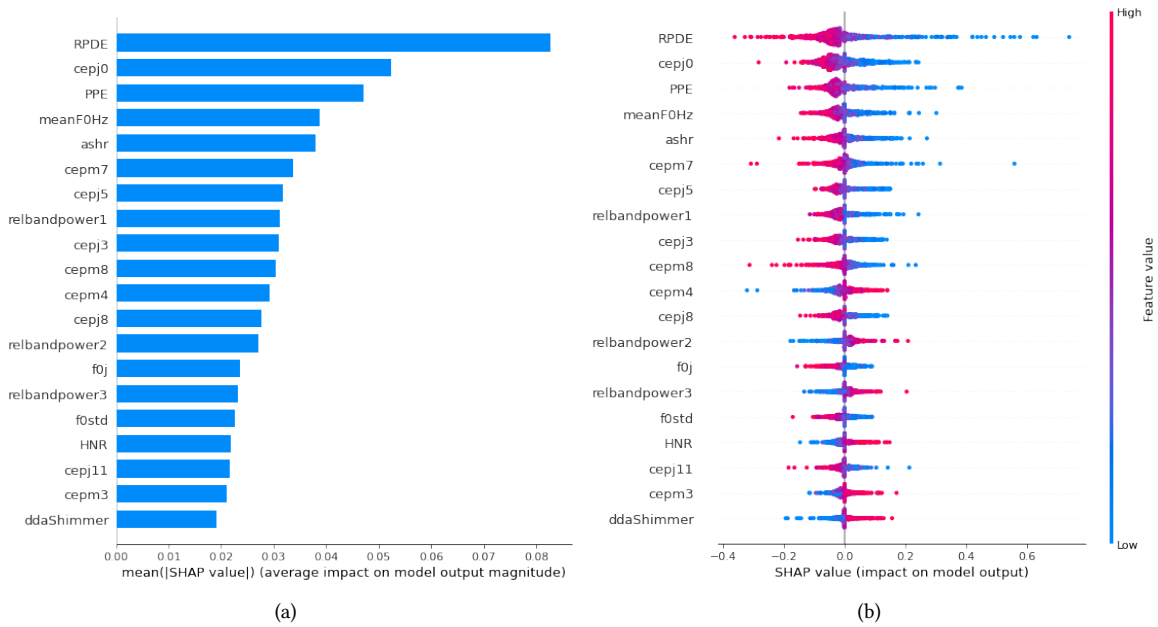


Fig. 7. SHAP for Age-matched model: This figure depicts the most important features for the model using the Age-matched data by plotting the SHAP values of every feature in every data sample. Plot (a) arranges the features in two steps: (i) Sorts features by the sum of SHAP value magnitudes over all samples, (ii) Uses SHAP values to show how each feature impacts the model's output: red color represents high value of a feature, blue represents low. For example, higher values of the feature cepm13 (the second to last one) increases the model's output value (b) Sorts all features by their mean absolute value to create a standard bar plot. From both plots, we see that two dysphonia related features: RPDE (measuring uncertainty in F0 estimation) and PPE (measure of inability of maintaining a constant F0) are regarded as the most important features. Apart from that, the most impactful features are usually the MFCC features : mean MFCC values in each channel is represented by the prefix cepm and the variation in those channels by cepj. Apart from that features like HNR (Harmonic to noise ratio), ashhr (median in amplitude perturbation), relative-band-power features (relbandpower1 ,relabandpower2 and relbandpower3 (amount of power in the frequency range 0.5-1kHz, 1kHz - 2kHz and 2kHz-4kHz) also impact the model's behaviour. Besides, there are some influence from the Pitch related features as well (meanF0Hz,f0j,f0std) as well. Please refer to Table 2 for a complete list of features and 4.3 for a detailed description of features.

29², Muhammad ali has PD by 42³. Through a focused group discussion, we have discovered that most of the members of our research group knows people who had PD below 40. In our dataset, there is also a minority of PD patients below the age of 50¹. Based on these observations, we believe that our system should provide access to all people irrespective of age. PD does not discriminate by age while attacking a person, and we should not discriminate based on age to provide equitable service to people of all age.

However, as these factors can work as confounded in PD analysis, we have decided to provide additional analysis to ensure that our model is not using the idiosyncrasies of group-specific information to make prediction and working reasonably well on all groups.

²<https://www.michaeljfox.org/michaels-story>

³<https://parkinsonsnewstoday.com/2016/06/10/muhammad-alis-advocacy-parkinsons-disease-endures-boxing-legacy/>

2.5.1 Our Model's performance on Gender-stratified and age matched test-set. We separately analyzed the performance of our models trained on Acoustic-features presented in Table 3 on three different data-sets: Male subjects, Female subjects and Age-matched subjects – created by removing all subjects below the age of 50. The result is presented in Table 6. We would like to reiterate that we did not train any model for this purpose. We just analyzed how our previous models are working on different population groups.

From Table 6, we can see that the best model's in each of Male and Age-matched domains have similar or better performance to the overall model's mentioned in Table 3 in terms of AUC. However, the model performs worse for Female subjects in comparison to all subjects. As we can see from the demographics information in Table. 1, females are over-represented in the Non-PD group and under-represented in the PD group. Previous Epidemiological studies have shown that both incidence and prevalence of PD are 1.5–2 times higher in men than in women [15, 48]. Therefore, we are more likely to get PD data-samples from male than female. To improve our model's performance, we plan to include more female PD subjects in our dataset in future.

2.5.2 Building specialized models for each gender and age-matched analysis. In this section, we report the performance of models trained exclusively on Male, Female and Age-matched dataset in Table 7. By comparing the performance with that presented in Table 3, we can see that the best models that used Male or Age-matched datasets performed in-par or better than the models using complete data. However, there is a performance drop for the models using Female dataset. As explained in the previous section, it may be caused by the data imbalance that is prevalent in the Female dataset.

We also analyzed the features that are driving these specialized models' performance through SHAP analysis. Fig 6 displays the most salient features ranked by their SHAP value and the distribution of how each feature impacts the model's decision making. We can see that the most important features are still dominated by the MFCC related features or complex features like HNR (Harmomic-to-Noise Ratio), relative-band-power in different frequency ranges (relbandpower1, relbandpower3), RPDE (uncertainty in F0 estimation), perturbation in F0 (ddpJitter) or Perturbation in amplitude (apq11Shimmer). However, one noticeable fact is that three pitch and jitter related features: median frequency (f0m), Standard-deviation in F0 (f0std) and median variation in F0 (f0jr) are also impacting the model's prediction which was not noticed in the SHAP analysis run on the All-data-model. According to SHAP, higher value of median frequency (f0m), higher median variation in F0 (f0jr), and lower standard-deviation in F0 (f0std) will push the model towards screening someone as a PD patient.

Similarly, we interpreted the salient features for the Age-matched dataset in Fig 7. We also notice that the most salient features are usually coming from the MFCC feature-groups, complex features(RPDE, PPE, HNR), relative-band-power (relbandpower1, relbandpower2, relbandpower3), and pitch related features. We also see that the pitch related features are also driving the model's prediction as well.

3 DISCUSSION AND FUTURE WORK

In this paper, we have worked with speech data collected largely from home-environment of subjects to predict PD. Due to collecting data from home, the data is very noisy and posits a lot of different challenges: lower audio quality, incomplete compliance with the the instructions, background noise, variety in recording devices, etc. We have showed that our model can perform well in this noisy environment and can achieve 0.75 AUC for by incorporating subjects of diverse age, gender and country. We have deployed interpretation techniques to explain our model's decision making criteria and demonstrated that our model emphasizes on the previously well established MFCC features and a sub-set of dysphonia features that were proven to be successful on the PD detection from verbal phonation task of pronouncing "AHHH" [25, 46]. Furthermore, we have conducted separate analysis on Male, Female and Age-matched groups. Our models have competitive performance on the Male and Age-matched group. We also built specialized models for each of these three groups: Male, Female and Age-matched and showed that they also perform as par the main model – except for the Female dataset. We

believe this disparity in performance is arising from the imbalance in Female dataset: a shortcoming we plan to address in future.

Although, our audio task is scripted, it is easy to perform for everyone and does not require specific instructions that are central to performing the verbal phonation task correctly. It opens the door for analyzing PD from non-scripted, regular speech in the future.

Besides, we also demonstrate that although our models are influenced by the RPDE, PPE and HNR features, they often do not behave as intuitively as they did in the PD detection task from Verbal phonation [25]. It opens up the opportunity to design specialized features that can capture useful properties of acoustic signals for a longer duration speech in the future.

4 METHODS

4.1 Data Collection

Our dataset is collected using the Parkinson's Analysis with Remote Kinetic-tasks (PARK) [24] – a web-browser based tool that guides a user to conduct a series of motor, facial expression and speech tasks following the MDS-UPDRS PD assessment protocol [14]. The conducted tasks are recorded via webcam and speaker connected to the PC/Laptop and uploaded to a server. Of all those recorded tasks, we select a task where the participants were instructed to read the sentences – *"The quick brown fox jumps over the lazy dog. The dog wakes up and follows the fox into the forest, but again the quick brown fox jumps over the lazy dog"*. The first sentence is a pangram: it contains all the letters of the English alphabet; thus we get features relevant for pronouncing all phonemes for each subject.

By extending the PARK protocol, a new protocol named Super-PARK was developed. The subjects, both PD patients and Non-PD patients, visited a local clinic where they were instructed by a trained doctor/technician to conduct all the a MDS-UPDRS tasks. Although the data is collected using the same web interface, an external camera is used for recording subjects. Due to in-person instruction and controlled data-collection environment, the Super-PARK data quality can be perceived as better than its PARK counterpart. We have built our primary models by incorporating data from both PARK and Super-PARK. However, to make sure that our model can perform well on the data collected in the home environment of our subjects, we have conducted two additional sets of analysis by removing the Super-PARK data from the test-data and then from both training and test-data altogether. Table 1 describes the demography of our subjects in a nutshell. Figure 1 shows the age distributions of the subjects.

4.2 Data Pre-processing

Since the data are collected by the users themselves in the privacy of their home, there are videos which are completely silent due to a dysfunctional/muted microphone in the users' end. We manually went through the videos and removed all absolutely silent audio files. there are often silence or noise at the beginning or end of the videos which can add additional difficulty for the machine learning algorithms.

Additionally, the subjects may often take some time to start pronouncing the task sentences. After completing the task, they often take additional time before stopping the recording. Hence, we have a substantial amount of noisy and irrelevant data at the beginning and ending of most of the data instances. To remove those irrelevant data, we use Penn Phonetics Lab Forced Aligner Toolkit (P2FA) ⁴ toolkit. Given a audio file and transcript, it tries to predict the time boundaries where each of the words in the transcript was pronounced. If it cannot recognize a set of words, it skips them and outputs time boundaries for the words it could recognize successfully. The toolkit is built on the research done in [50], where they apply a combination of Hidden Markov Models (from The

⁴https://github.com/jaekookang/p2fa_py3

Hidden Markov Model Toolkit (HTK) ⁵) and Gaussian-Mixture-Models(GMM) to align the words with the audio. The processing is done in several stages: HMM based models output the most likely sequence of hidden states for a given audio; Those hidden states are combined into phonemes and those phonemes are combined into words using a predefined dictionary (comprised of words and their corresponding phoneme pattern) through GMM based models.

From the output of this system, we can get the starting time of first word that was recognized by the P2FA and the ending time of the last word recognized by P2FA. We use the audio segment in between them for further analysis. For building models capable of predicting PDP, we extract two different sets of features: Acoustic-Features (4.3) and Embedding-features (4.4)

4.3 Standard Features Extraction

We extracted features by combining a subset of features collected through several sources: PRAAT features [6] through the Parselmouth [19] python interface and the previously used features relevant for PDP analysis in [25, 26, 46]. After calculating all the features, we constructed a correlation matrix of the feature values to calculate the degree of correlation between the features. Then, we iterated over each pair of features in an un-ordered fashion, and if the correlation co-efficient between them was over .9, we dropped one of those features from further analysis. Table 2 contains a short overview of the features used in our analysis; the feature names with an asterisk (*) are the ones used for building the models. We provide a more comprehensive description of the features in the following sections. Some of our definitions are adapted from the official PRAAT documentation ⁶.

4.3.1 Pitch Related Features: Pitch denotes the rate of vibrations present in a sound **f0m** denotes the median fundamental frequency or pitch of the audio signal. **f0std** denotes the standard deviation of fundamental frequency **f0**.

4.3.2 Jitter related features: Jitter defines how much a signal deviates from its presumed true periodicity; it is often an undesired quantity if our signals are assumed to be periodic. **f0j** is the measure of jitter collected by calculating the mean variation of **f0**. **f0jr** is the jitter measure calculated using the median variation of **f0**. **localjitter** denotes the average of the absolute differences between consecutive period of a signal – divided by the average period. **rapJitter** – Relative Average Perturbation– is computed by the average absolute difference between a period and the average of that period and the two neighbouring periods; divided by the average period. **ppq5Jitter** denotes the five-point Period Perturbation Quotient: the average absolute difference between a period and the average of it and its four closest neighbours – divide by the average period. **ddpJitter** denotes the average absolute difference between consecutive differences between consecutive periods, divided by the average period.

4.3.3 Shimmer Related Features: Shimmer is a measurement of amplitude instability in an audio signal; a normal voice will have minimal instability during sustained verbal phonation production. **ash** is the Shimmer value by quantifying the mean variation of amplitude in voice signals. **ashr** is the Shimmer calculated using the median variation of amplitude. **localShimmer** calculates the average absolute difference between the amplitude of the consecutive periods in a signal divided by the average amplitude. **localDBShimmer** is the average of the absolute value of 10-based logarithm of the difference between the amplitudes of consecutive periods in the signal, multiplied by 20. **apq3Shimmer** is the three-point Amplitude Perturbation Quotient: the average absolute difference between the amplitude of a period and the average of the amplitudes of its two neighbours – left and right – divided by the average amplitude. **apq5Shimmer** and **apq11Shimmer** are similar to **apq3Shimmer**,

⁵<http://htk.eng.cam.ac.uk/>

⁶<https://www.fon.hum.uva.nl/praat/>

but uses data from four and 10 neighbours respectively instead of two. **ddpShimmer** is three times the value of **apq3Shimmer**

4.3.4 MFCC: Mel Frequency Cepstral Coefficients (MFCC) [34] are used to understand the rate of energy changes in different spectrum bands of the speech: If a cepstral coefficient has negative value, it indicates that majority of spectral energy in that spectrum band is concentrated in the high frequencies; if a cepstral has positive value, it indicates that majority of spectral energy is concentrated in low frequencies. As we get several entries for each of the 13 spectral regions of MFCC, we take the mean (**cemp[0-12]**) and mean variation (**cepj[0-12]**) for each of these spectral regions.

4.3.5 Relative Band Power: Relative band power features were calculated by checking how much power is present in four different spectrum of frequency windows in the range [0,500,1000,2000,4000] Hz. The power contained in these four regions are denoted by **relbandpower[0-3]**. Through applying FFT, we convert the audio signal into frequency domain. Then, we calculate the power contained in the frequencies belonging to each bucket, aggregate them and calculate the median in each of these buckets

4.3.6 Harmonic-to-noise(HNR) ratio. HNR denotes the ratio of desired signal and background noise; higher HNR indicates better quality of audio.

4.3.7 Recurrence period density entropy (RPDE): A perfectly recurrent time signal will maintain a strict time period. Recurrence period density entropy (RPDE) determines how much a signal is maintaining a strict periodicity after the signal is reconstructed in phase space [26]. By aggregating the time-periods recorded in our signal, and calculating the entropy of those time-periods, we get a measure of how much variation is present in those time-periods. A perfectly healthy voice will be able to maintain sustained vibration, hence it should have an entropy close to zero. Finally, the RPDE values are normalized in the range [0,1] to be used as feature.

4.3.8 Detrended fluctuation analysis (DFA): As human voice is produced by turbulent air-flows through our vocal folds, degeneration of voice-fold structure (due to age or diseases) can produce increased noise in speech [26]. Detrended fluctuation analysis (DFA) measures the extent of the stochastic self-similarity of the noise in the speech signal produced due to possible alteration in vocal fold structure. These kind of noises can be represented through a statistical scaling component on a range of physical scales; this scaling component is comparatively larger for people with voice disorders [25, 26].

4.3.9 Pitch Period Entropy (PPE): [25] introduces a new feature Pitch Period Entropy (PPE) to calculate the entropy present in the pitch of an audio signal. First, a standard time-signal of pitch is converted into the logarithmic domain to capture the logarithmic nature of speech generation and perception. Then, to remove the gender and person specific trends present in the pitch – as we know that females have higher pitch than man, and there exists individual differences in pitch – we apply a standard whitening filter. Then, we use calculate the probability density of the residual signal. For a healthy voice signal, most of the probabilities will be concentrated on a narrow range. However, the people with vocal disorders cannot maintain a sustained pitch for a long time, therefore, there probability distribution will be much more dispersed. This dispersion is calculated through entropy, which precisely calculates how much disorganization there is in a system. A lower entropy means that the pitch was sustained over a long time, an higher entropy indicates problems with the vocal cords and probably dysphonia as well.

4.4 Embedding-features Extraction

We extracted Problem Agnostic Speech Encoder (PASE) embeddings [33] for our audio files. PASE represents the information contained in a raw audio instance through a list of encoded vectors. To make sure that the encoded vectors contain the same information as the input audio file, they decode various properties of the audio file which

include, the audio waveform, the Log Power Spectrum, Mel-frequency cepstral coefficients (MFCC), four prosody features (interpolated logarithm of the fundamental frequency, voiced/unvoiced probability, zero-crossing rate, and energy), Local Info max, etc. from the encoded vectors. To decode all these properties successfully, the encoded vectors must retain the relevant information about the input audio file. As these properties represent the inherent characteristics of the input audio file rather than any task-specific features, they can be easily used to solve a host of downstream tasks like speech classification, speaker recognition, emotion recognition and as we demonstrate, PD detection.

4.5 Experiments

For each of the feature sets, we applied a standard set of machine learning algorithms like Support-vector-machine (SVM) [9], XGBoost [8], LightGBM [20], and Random-Forest [17] Classifier to classify PD vs. Non-PD. SVM separates out the data into several classes while maintaining a maximum possible margin among the classes. It can use the kernel trick to project the data on a more abstract hyper-plane and thus provide the model with more expressiveness. Random forest is built as an ensemble of Decision Trees; each decision tree builds a tree using a subset of features and learns if-else type decision rules to make a prediction. We also use XGBoost and LightGBM: two algorithms based on Gradient boosting where they build successively better models by refining the current models. eXtreme Gradient Boosting(XGBoost) provides a framework for fast, distributed gradient boosting while employing sophisticated heuristics for penalizing poorly performing trees and better use of regularization. LightGBM is a boosting algorithm that employs leaf-wise tree growth and hence it can make a better estimation of the information gain through examining a smaller subset of data, and gain very equivalent accuracy very fast at the expense of lower memory usage.

We used a leave-one-out cross validation training strategy; using this strategy one sample of the dataset is left out and the other $n-1$ samples are used to create a model and predict the remaining sample. We used metrics like Binary Accuracy and AUC to report our model's performance. Area-Under-Curve (AUC) is the area under the ROC (Receiver Operating Characteristics) curve. The ROC curve is constructed by taking the ratio of the True-Positive-Rate and the False-Positive-Rate by varying while varying the threshold of the decision. AUC can have highest value of 1, which denotes that the two classes can be separated perfectly; whereas an AUC value of 0.5 indicates that the model has no capability to distinguish between the two classes⁷. Since our dataset is imbalanced, AUC is a much better metric to understand the true performance of our model.

Since there exists significant imbalance between our PD and Non-PD class and PD is the minority class, we have much more samples of Non-PD than PD. Therefore, the model has a tendency to choose the majority Non-PD class as a default which can yield a high False-Negative score, which is particularly bad in our case since our system is envisioned to be screening tool to help people get a preliminary screening for PD so that they can visit a doctor immediately. It will be really problematic if we predict a PD patient as Non-Pd and thus provide him/her with a false sense of security and create a situation where his/her disease progress due to lack of medical care. To tackle that challenge, we used the Synthetic Minority Oversampling Technique (SMOTE) [7] and SVMsmote [32]. SMOTE can create synthetic data instances for the under-represented class. For each sample in the minority class, it calculates the K-nearest neighbours of that instance. Then, it calculates the straight line connecting each sample to all of its neighbours and then samples new synthetic data samples situated over that connecting line. SVMsmote focuses on the boundary of different classes. We know that SVM creates a decision boundary around classes by trying to maintain the maximum possible margin among classes. Thus SVMsmote samples data in a manner than focuses on the boundary region of the minority class and samples data from that region such that the boundary between the classes is either expanded or consolidated.

⁷<https://towardsdatascience.com/understanding-auc-roc-curve-68b2303cc9c5>

4.6 Model Interpretation

For interpreting the models, we are using the SHAP technique based on Shapley Value. Shapley value is a game-theoretic concept of distributing the payout fairly among the players [38]. In the machine learning context, each individual feature of an instance can be thought of as a player and the payout is the difference between an instance's prediction and average prediction. It is based on rigorous mathematical foundation and it ensures fair distribution of importance amongst the features through ensuring four key mathematical properties: Efficiency, Symmetry, Dummy and Additivity.

To compute the shapely value, [40] computes the average marginal contribution for each feature across all the examples. For each feature, all possible combination of all the other features – defined as coalition – is generated. Then for each samples generated from those coalitions, two kinds of scores are calculated: one where the intended feature is positive and another where it is not. The weighted average of the difference between these two scores is the Shapley Value.

Lundberg et al 2017 [30] proposed SHAP(SHapley Additive exPlanations) based on Shapley Value with several additions. They added two methods called KernelSHAP that estimates Shapley values through kernel-based estimation and TreeSHAP that provides an exact, efficient estimation method for tree-based models like Decision Tree, Random Forest, etc. SHAP unifies the idea of Local interpretable model-agnostic explanations (LIME) and Shapley value by enabling us to build both local and global models.

Lundberg et al. 2020 [29] introduced methods to advance shap into the gradient boosting and tree based models like decision trees. They provided a polynomial time model to compute optimized explanations. Their method can generate local interpretations – how the features impact one particular prediction – and then combine those local interpretations to make global interpretations about features present in the entire dataset impact on the model's decision. Their method can give Feature Dependence, interaction effects, model summarization among many other things. By setting up a class of features to condition on, they traverse the tree in the following manner: if we are traversing on a node that was split based on a feature we are conditioning on, we simply follow the decision path; otherwise, the results from the left and right sub-trees originating from the current node is computed recursively and their results added through a weighted summation strategy. They validated their approach on three classical medical dataset – modeling mortality risk from 20 years of follow up through National Health and Nutrition Examination Survey (NHANES) I Epidemiologic Followup Study, classifying whether kidney patients will develop acute end-state renal diseases with 4 year through Chronic Renal Insufficiency Cohort (CRIC) study and predicting duration of hospital stay of a patient after an upcoming procedure. Their models achieved competitive baseline performance while their explanations provided interpretable insights about the model's decision making process that is grounded in previous research.

5 DATA AND CODE AVAILABILITY

Please contact the corresponding author for getting access to the data and code. The maintenance and sharing of data collected through the PARK system must adhere to the Health Insurance Portability and Accountability Act (HIPPA) regulations. Therefore, it can only be shared by adding the interested party in the protocol maintained by the relevant Institutional Review Board (IRB).

REFERENCES

- [1] [n.d.]. EARLY ONSET PARKINSON'S DISEASE. <https://www.apdaparkinson.org/what-is-parkinsons/early-onset-parkinsons-disease/>. Accessed: 2020-08-26.
- [2] Mohammad Rafayet Ali, Javier Hernandez, E Ray Dorsey, Ehsan Hoque, and Daniel McDuff. [n.d.]. Spatio-Temporal Attention and Magnification for Classification of Parkinson's Disease from Videos Collected via the Internet. In *2020 15th IEEE International Conference on Automatic Face and Gesture Recognition (FG 2020)(FG)*. 53–60.

- [3] S. Arora, V. Venkataraman, A. Zhan, S. Donohue, K.M. Biglan, E.R. Dorsey, and M.A. Little. 2015. Detecting and monitoring the symptoms of Parkinson's disease using smartphones: A pilot study. *Parkinsonism and Related Disorders* 21, 6 (June 2015), 650–653. <https://doi.org/10.1016/j.parkreldis.2015.02.026>
- [4] Andrea Bandini, Silvia Orlandi, Hugo Jair Escalante, Fabio Giovannelli, Massimo Cincotta, Carlos A Reyes-Garcia, Paola Vanni, Gaetano Zaccara, and Claudia Manfredi. 2017. Analysis of facial expressions in Parkinson's disease through video-based automatic methods. *Journal of neuroscience methods* 281 (2017), 7–20.
- [5] Kritagya Bhattarai, PWC Prasad, Abeer Alsadoon, L Pham, and Amr Elchouemi. 2017. Experiments on the MFCC application in speaker recognition using Matlab. In *2017 Seventh International Conference on Information Science and Technology (ICIST)*. IEEE, 32–37.
- [6] Paul Boersma and David Weenink. 2018. Praat: doing phonetics by computer [Computer program]. Version 6.0.37, retrieved 3 February 2018 <http://www.praat.org/>.
- [7] Nitesh V Chawla, Kevin W Bowyer, Lawrence O Hall, and W Philip Kegelmeyer. 2002. SMOTE: synthetic minority over-sampling technique. *Journal of artificial intelligence research* 16 (2002), 321–357.
- [8] Tianqi Chen and Carlos Guestrin. 2016. Xgboost: A scalable tree boosting system. In *Proceedings of the 22nd acm sigkdd international conference on knowledge discovery and data mining*. ACM, 785–794.
- [9] Corinna Cortes and Vladimir Vapnik. 1995. Support-vector networks. *Machine learning* 20, 3 (1995), 273–297.
- [10] Namrata Dave. 2013. Feature extraction methods LPC, PLP and MFCC in speech recognition. *International journal for advance research in engineering and technology* 1, 6 (2013), 1–4.
- [11] MC de De Rijk, LJ Launer, K Berger, MM Breteler, JF Dartigues, M Baldereschi, L Fratiglioni, A Lobo, J Martinez-Lage, C Trenkwalder, et al. 2000. Prevalence of Parkinson's disease in Europe: A collaborative study of population-based cohorts. Neurologic Diseases in the Elderly Research Group. *Neurology* 54, 11 Suppl 5 (2000), S21–3.
- [12] Joseph R Duffy. 2019. *Motor Speech Disorders E-Book: Substrates, Differential Diagnosis, and Management*. Elsevier Health Sciences.
- [13] Gary J Gates. 2011. How many people are lesbian, gay, bisexual and transgender? (2011).
- [14] Christopher G Goetz, Barbara C Tilley, Stephanie R Shaftman, Glenn T Stebbins, Stanley Fahn, Pablo Martinez-Martin, Werner Poewe, Cristina Sampaio, Matthew B Stern, Richard Dodel, et al. 2008. Movement Disorder Society-sponsored revision of the Unified Parkinson's Disease Rating Scale (MDS-UPDRS): scale presentation and clinimetric testing results. *Movement disorders: official journal of the Movement Disorder Society* 23, 15 (2008), 2129–2170.
- [15] Charlotte A Haaxma, Bastiaan R Bloem, George F Borm, Wim JG Oyen, Klaus L Leenders, Silvia Eshuis, Jan Booij, Dean E Dluzen, and Martin WIM Horstink. 2007. Gender differences in Parkinson's disease. *Journal of Neurology, Neurosurgery & Psychiatry* 78, 8 (2007), 819–824.
- [16] Aileen K Ho, Robert Insek, Caterina Marigliani, John L Bradshaw, and Sandra Gates. 1998. Speech impairment in a large sample of patients with Parkinson's disease. *Behavioural neurology* 11, 3 (1998), 131–137.
- [17] Tin Kam Ho. 1995. Random decision forests. In *Proceedings of 3rd international conference on document analysis and recognition*, Vol. 1. IEEE, 278–282.
- [18] Daniel H Jacobs, Jeffrey Shuren, Dawn Bowers, and Kenneth M Heilman. 1995. Emotional facial imagery, perception, and expression in Parkinson's disease. *Neurology* 45, 9 (1995), 1696–1702.
- [19] Yannick Jadoul, Bill Thompson, and Bart de Boer. 2018. Introducing Parselmouth: A Python interface to Praat. *Journal of Phonetics* 71 (2018), 1–15. <https://doi.org/10.1016/j.wocn.2018.07.001>
- [20] Guolin Ke, Qi Meng, Thomas Finley, Taifeng Wang, Wei Chen, Weidong Ma, Qiwei Ye, and Tie-Yan Liu. 2017. Lightgbm: A highly efficient gradient boosting decision tree. In *Advances in neural information processing systems*. 3146–3154.
- [21] SV Khadilkar. 2013. Neurology in India. *Annals of Indian Academy of Neurology* 16, 4 (2013), 465.
- [22] Tomi Kinnunen, Evgenia Chernenko, Marko Tuononen, Pasi Fränti, and Haizhou Li. 2007. Voice activity detection using MFCC features and support vector machine. In *Int. Conf. on Speech and Computer (SPECOM07)*, Moscow, Russia, Vol. 2. 556–561.
- [23] Anthony E Lang and Andres M Lozano. 1998. Medical Progress: Parkinson's Disease First of Two Parts. *The New England Journal of Medicine* 339, 15 (1998), 1044–1053.
- [24] Raina Langevin, Mohammad Rafayet Ali, Taylan Sen, Christopher Snyder, Taylor Myers, E Dorsey, and Mohammed Ehsan Hoque. 2019. The PARK Framework for Automated Analysis of Parkinson's Disease Characteristics. *Proceedings of the ACM on Interactive, Mobile, Wearable and Ubiquitous Technologies* 3, 2 (2019), 54.
- [25] Max Little, Patrick McSharry, Eric Hunter, Jennifer Spielman, and Lorraine Ramig. 2008. Suitability of dysphonia measurements for telemonitoring of Parkinson's disease. *Nature Precedings* (2008), 1–1.
- [26] Max A Little, Patrick E McSharry, Stephen J Roberts, Declan AE Costello, and Irene M Moroz. 2007. Exploiting nonlinear recurrence and fractal scaling properties for voice disorder detection. *Biomedical engineering online* 6, 1 (2007), 23.
- [27] Jeri A Logemann, Hilda B Fisher, Benjamin Boshes, and E Richard Blonsky. 1978. Frequency and cooccurrence of vocal tract dysfunctions in the speech of a large sample of Parkinson patients. *Journal of Speech and hearing Disorders* 43, 1 (1978), 47–57.
- [28] Luca Lonini, Andrew Dai, Nicholas Shawen, Tanya Simuni, Cynthia Poon, Leo Shimanovich, Margaret Daeschler, Roozbeh Ghaffari, John A Rogers, and Arun Jayaraman. 2018. Wearable sensors for Parkinson's disease: which data are worth collecting for training

- symptom detection models. *npj Digital Medicine* 1 (2018), 64.
- [29] Scott M Lundberg, Gabriel Erion, Hugh Chen, Alex DeGrave, Jordan M Prutkin, Bala Nair, Ronit Katz, Jonathan Himmelfarb, Nisha Bansal, and Su-In Lee. 2020. From local explanations to global understanding with explainable AI for trees. *Nature machine intelligence* 2, 1 (2020), 2522–5839.
- [30] Scott M Lundberg and Su-In Lee. 2017. A unified approach to interpreting model predictions. In *Advances in Neural Information Processing Systems*. 4765–4774.
- [31] Meinard Müller. 2007. *Information retrieval for music and motion*. Vol. 2. Springer.
- [32] Hien M Nguyen, Eric W Cooper, and Katsuari Kamei. 2011. Borderline over-sampling for imbalanced data classification. *International Journal of Knowledge Engineering and Soft Data Paradigms* 3, 1 (2011), 4–21.
- [33] Santiago Pascual, Mirco Ravanelli, Joan Serrà, Antonio Bonafonte, and Yoshua Bengio. 2019. Learning Problem-Agnostic Speech Representations from Multiple Self-Supervised Tasks. In *Proc. of the Conf. of the Int. Speech Communication Association (INTERSPEECH)*. 161–165. <http://dx.doi.org/10.21437/Interspeech.2019-2605>
- [34] Louis CW Pols et al. 1977. Spectral analysis and identification of Dutch vowels in monosyllabic words. (1977).
- [35] Amir Hossein Poorjam, Mathew Shaji Kavalekalam, Liming Shi, Yordan P Raykov, Jesper Rindom Jensen, Max A Little, and Mads Græsbøll Christensen. 2019. Automatic Quality Control and Enhancement for Voice-Based Remote Parkinson's Disease Detection. *arXiv preprint arXiv:1905.11785* (2019).
- [36] Alice Rueda and Sridhar Krishnan. 2017. Feature analysis of dysphonia speech for monitoring Parkinson's disease. In *2017 39th Annual International Conference of the IEEE Engineering in Medicine and Biology Society (EMBC)*. IEEE, 2308–2311.
- [37] Aa Schrag, YB Ben-Shlomo, and Niall Quinn. 2002. How valid is the clinical diagnosis of Parkinson's disease in the community? *Journal of Neurology, Neurosurgery & Psychiatry* 73, 5 (2002), 529–534.
- [38] Lloyd S Shapley. 1953. A value for n-person games. *Contributions to the Theory of Games* 2, 28 (1953), 307–317.
- [39] Neha Singh, Viness Pillay, and Yahya E Choonara. 2007. Advances in the treatment of Parkinson's disease. *Progress in neurobiology* 81, 1 (2007), 29–44.
- [40] Erik Štrumbelj and Igor Kononenko. 2014. Explaining prediction models and individual predictions with feature contributions. *Knowledge and information systems* 41, 3 (2014), 647–665.
- [41] Linda Tickle-Degnen and Kathleen Doyle Lyons. 2004. Practitioners' impressions of patients with Parkinson's disease: the social ecology of the expressive mask. *Social Science & Medicine* 58, 3 (2004), 603–614.
- [42] Ingo R Titze and Daniel W Martin. 1998. Principles of voice production.
- [43] Athanasios Tsanas, Max A Little, Patrick E McSharry, and Lorraine O Ramig. 2009. Accurate telemonitoring of Parkinson's disease progression by noninvasive speech tests. *IEEE transactions on Biomedical Engineering* 57, 4 (2009), 884–893.
- [44] Athanasios Tsanas, Max A Little, Patrick E McSharry, and Lorraine O Ramig. 2011. Nonlinear speech analysis algorithms mapped to a standard metric achieve clinically useful quantification of average Parkinson's disease symptom severity. *Journal of the royal society interface* 8, 59 (2011), 842–855.
- [45] Athanasios Tsanas, Max A Little, Patrick E McSharry, and Lorraine O Ramig. 2012. Using the cellular mobile telephone network to remotely monitor parkinsons disease symptom severity. *IEEE Transactions on Biomedical Engineering* 9 (2012).
- [46] Athanasios Tsanas, Max A Little, Patrick E McSharry, Jennifer Spielman, and Lorraine O Ramig. 2012. Novel speech signal processing algorithms for high-accuracy classification of Parkinson's disease. *IEEE transactions on biomedical engineering* 59, 5 (2012), 1264–1271.
- [47] Alexandros T. Tzallas, Markos G. Tsipouras, Georgios Rigas, Dimitrios G. Tsilikakis, Evaggelos C. Karvounis, Maria Chondrogiorgi, Fotis Psomadellis, Jorge Cancela, Matteo Pastorino, Maria Teresa Arredondo Waldmeyer, Spiros Konitsiotis, and Dimitrios I. Fotiadis. 2014. PERFORM: A System for Monitoring, Assessment and Management of Patients with Parkinson's Disease. *Sensors (Basel)* 14, 11 (Nov. 2014), 21329–21357. <https://doi.org/10.3390/s141121329>
- [48] Stephen K Van Den Eeden, Caroline M Tanner, Allan L Bernstein, Robin D Fross, Amethyst Leimpeter, Daniel A Bloch, and Lorene M Nelson. 2003. Incidence of Parkinson's disease: variation by age, gender, and race/ethnicity. *American journal of epidemiology* 157, 11 (2003), 1015–1022.
- [49] Peng Wu, Isabel Gonzalez, Georgios Patsis, Dongmei Jiang, Hichem Sahli, Eric Kerckhofs, and Marie Vandekerckhove. 2014. Objectifying facial expressivity assessment of Parkinson's patients: preliminary study. *Computational and mathematical methods in medicine* 2014 (2014).
- [50] Jiahong Yuan and Mark Liberman. 2008. Speaker identification on the SCOTUS corpus. *Journal of the Acoustical Society of America* 123, 5 (2008), 3878.